Neuro-Oncology 14(8):1079–1089, 2012.
doi:10.1093/neuonc/nos141
Advance Access publication June 18, 2012

^{18}F-FDOPA and ^{18}F-FLT positron emission tomography parametric response maps predict response in recurrent malignant gliomas treated with bevacizumab

Robert J. Harris, Timothy F. Cloughesy, Whitney B. Pope, Phioanh L. Nghiemphu, Albert Lai, Taryar Zaw, Johannes Czernin, Michael E. Phelps, Wei Chen, and Benjamin M. Ellingson

Departments of Radiological Sciences (R.J.H., W.B.P., T.Z., B.M.E.), Biomedical Physics (R.J.H., B.M.E.), Neurology (T.F.C., P.L.N., A.L.), and Molecular and Medical Pharmacology (J.C., W.C., M.E.P.), David Geffen School of Medicine, University of California Los Angeles, Los Angeles, California

The current study examined the use of voxel-wise changes in ^{18}F-FDOPA and ^{18}F-FLT PET uptake, referred to as parametric response maps (PRMs), to determine whether they were predictive of response to bevacizumab in patients with recurrent malignant gliomas. Twenty-four patients with recurrent malignant gliomas who underwent bevacizumab treatment were analyzed. Patients had MR and PET images acquired before and at 2 time points after bevacizumab treatment. PRMs were created by examining the percentage change in tracer uptake between time points in each image voxel. Voxel-wise increase in PET uptake in areas of pretreatment contrast enhancement defined by MRI stratified 3-month progression-free survival (PFS) and 6-month overall survival (OS) according to receiver-operating characteristic curve analysis. A decrease in PET tracer uptake was associated with longer PFS and OS, whereas an increase in PET uptake was associated with short PFS and OS. The volume fraction of increased ^{18}F-FDOPA PET uptake between the 2 posttreatment time points also stratified long- and short-term PFS and OS (log-rank, $P < .05$); however, ^{18}F-FLT uptake did not stratify OS. This study suggests that an increase in FDOPA or FLT PET uptake on PRMs after bevacizumab treatment may be a useful biomarker for predicting PFS and that FDOPA PET PRMs are also predictive of OS in recurrent gliomas treated with bevacizumab.

Received February 20, 2012; accepted May 21, 2012.

Corresponding Author: Benjamin M. Ellingson, PhD, Assistant Professor, Department of Radiological Sciences, David Geffen School of Medicine, University of California Los Angeles, 924 Westwood Blvd., Ste. 615, Los Angeles, CA 90024 (bellingson@mednet.ucla.edu).

Keywords: Bevacizumab, 18F-FDOPA, 18F-FLT, glioblastoma, PRMs.

Malignant gliomas (World Health Organization [WHO] grades III–IV) are primary central nervous system (CNS) tumors with a poor patient prognosis. Malignant gliomas constitute approximately 70% of all neuroepithelial tumors and approximately 23% of all primary CNS tumors.[1] Despite new therapies, the median survival time for patients with malignant gliomas has improved only marginally. Bevacizumab, a humanized monoclonal antibody that inhibits vascular endothelial growth factor (VEGF), is now the standard of care for recurrent malignant gliomas, including glioblastoma.[2] Treatment with bevacizumab has shown to be effective in extending progression-free survival in patients with glioblastoma;[3] however, only a few biomarkers are available for predicting the response of recurrent malignant gliomas to bevacizumab therapy.[4–9]

Positron emission tomography (PET) imaging using [^{18}F]-fluorodeoxyglycose (FDG) is the most commonly used radiotracer method for examining metabolic activity of malignant tumors. Despite its widespread use in oncology, FDG often provides relatively poor contrast in the brain between background tissue and tumor because of high uptake in normal brain tissue.[10] [^{18}F]-fluoro-3-deoxy-3-L-fluorothymidine (^{18}F-FLT), a thymidine analog that is a surrogate marker for DNA synthesis based on the activity of thymidine kinase-1, has shown value in directly quantifying tumor cell proliferation.[11] Although the absolute uptake in tumor regions is typically lower for ^{18}F-FLT than for ^{18}F-fluorodeoxyglucose (^{18}F-FDG), the relative contrast

between tumor and normal tissue is higher for ^{18}F-FLT and has been shown to be more sensitive than ^{18}F-FDG for evaluating recurrent high-grade gliomas.[11] 3,4-dihydroxy-6-[^{18}F]-fluoro-L-phenylalanine (^{18}F-FDOPA) is an amino acid analog. Similar to ^{18}F-FLT, ^{18}F-FDOPA has also shown improved contrast between tumor and normal brain tissue in patients with high-grade glioma because of elevated amino acid transportation in malignant tumor cells.[12] We hypothesized that voxel-wise changes in ^{18}F-FDOPA and ^{18}F-FLT uptake, or parametric response maps (PRMs), in the same patient across multiple time points would be predictive of response in patients with recurrent glioblastoma treated with bevacizumab, as measured by progression-free (PFS) and overall survival (OS). Furthermore, we hypothesized that the combination of ^{18}F-FDOPA and ^{18}F-FLT would be synergistically prognostic, because the biological mechanisms of tracer uptake are fundamentally different.

To test these hypotheses, PET PRMs were constructed for both ^{18}F-FDOPA and ^{18}F-FLT for each patient in regions of contrast enhancement defined by magnetic resonance imaging (MRI). PRMs were calculated by examining the change in PET uptake before and after initial bevacizumab treatment, along with the change in PET uptake between the 2 time points after initiation of bevacizumab treatment.

Materials and Methods

Patients

All patients in this study signed institutional review board–approved informed consent to have their data collected and stored in our institution's neuro-oncology database. Data from 24 patients with malignant gliomas (WHO grade IV, $n = 18$; WHO grade III, $n = 6$) who were previously examined in separate studies using circular regions of interest and placed in the highest tumor standard uptake value (SUV)[13,14] were retrospectively analyzed for the current study. All patients were treated with bevacizumab, and all but 2 received a supplemental chemotherapeutic agent (irinotecan). Of the 24 patients in the study, ^{18}F-FDOPA data was acquired for 23, ^{18}F-FLT data was acquired for 21, and 20 received both ^{18}F-FDOPA and ^{18}F-FLT scans. PET time points were taken within 1 week before the start of bevacizumab treatment, 1–2 weeks after treatment, and 5–7 weeks after the start of treatment (Fig. 1). ^{18}F-FDOPA and ^{18}F-FLT scans were obtained within 1–2 days at each time point in patients with both scans, and the order of PET scan acquisition was randomized at each follow-up time.

PET

^{18}F-FDOPA images were acquired and processed using methods similar to those previously described.[15–17] ^{18}F-FDOPA was synthesized according to standard procedures[18,19] and injected at a dose of 1.1–6.6 MBq/kg body weight. ^{18}F-FLT was synthesized locally using previously described methods,[20] and ^{18}F-FLT images were acquired and processed using techniques similar to those previously described.[13] For both ^{18}F-FDOPA and ^{18}F-FLT images, a transmission scan was obtained for attenuation correction.[21] ^{18}F-FDOPA emission data were acquired in 3-dimensional mode 10 min after injection for a total of 30 min. Data collected at 10–30 min were summed to obtain a 20-min static ^{18}F-FDOPA image after reconstruction as previously described. ^{18}F-FLT emission data were collected in 3-dimensional mode immediately after injection for a total of 60 min. Data collected at 30–60 min were summed to obtain a 30-min static ^{18}F-FLT image and reconstructed as previously described. All images for both ^{18}F-FDOPA and ^{18}F-FLT were obtained using a high-resolution full-ring PET scanner (ECAT HR+; Siemens/CTI).

MRI

Data were collected on a 1.5T MR system (General Electric Medical Systems or Siemens Medical) using pulse sequences supplied by the scanner manufacturer. Standard anatomical MRI sequences included axial T1 weighted (TE/TR = 15 ms/400 ms, slice thickness = 5 mm with 1 mm interslice distance, NEX = 2, matrix size = 256 × 256, and FOV = 24 cm), T2 weighted FSE (TE/TR = 126–130 ms/4000 ms, slice thickness = 5 mm with 1 mm interslice distance, NEX = 2, matrix size = 256 × 256, and FOV = 24 cm), and fluid-attenuated inversion recovery (FLAIR) images (TI = 2200 ms, TE/TR = 120 ms/4000 ms, slice thickness = 5 mm with 1 mm interslice distance, NEX = 2, matrix

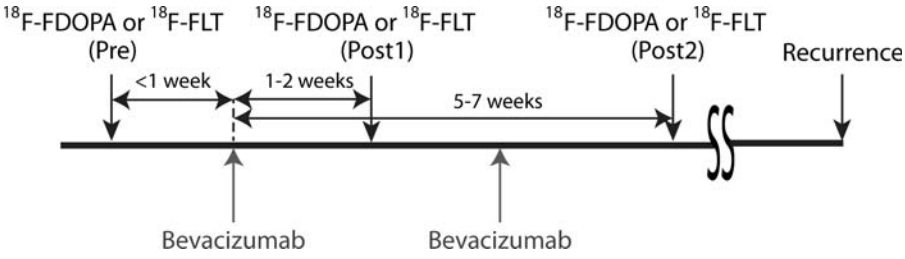

Fig. 1. Experimental timeline showing relative timing of bevacizumab treatment and PET image acquisition.

size = 256 × 256, and FOV = 24 cm). In addition, gadopentetate dimeglumine enhanced (Magnevist; Berlex; 0.1 mmol/kg) axial and coronal T1-weighted images (T1 + C; coronal: TE/TR = 15 ms/400 ms, slice thickness 3 mm with 1 mm interslice distance, NEX = 2, a matrix size of 256 × 256, and FOV = 24 cm) were acquired after contrast injection.

Image Registration

All images for each patient at each time point were registered to a high resolution (1.0 mm isotropic), T1-weighted brain atlas (MNI152; Montreal Neurological Institute) using a mutual information algorithm and a 12-degree of freedom transformation using FSL (FMRIB, Oxford, UK; http://www.fmrib.ox.ac.uk/fsl/). Manual adjustment, if necessary, was performed using the tkregister2 routine available from Freesurfer (surfer.nmr.mgh.harvard.edu; Massachusetts General Hospital, Harvard Medical School).

PET PRM Generation

PET SUV images for each patient and time point were normalized separately to an area of contralateral normal-appearing white matter (NAWM) for each patient. Areas of contralateral NAWM were selected from the corresponding aligned MR image acquired closest to the time of that PET image. PRMs of the relative percentage change in normalized voxel SUV values from one time point to the next were calculated for the pretreatment and first posttreatment time point ([Post1-Pre]/Pre) and the 2 posttreatment time points ([Post2-Post1]/Post1). After calculating the 2 sets of PRMs for each PET tracer, a histogram of PRM values in NAWM regions were calculated using values from all available patients. A 95% confidence interval of normal tissue PRM variability across time was calculated from these data, similar to other voxel-wise techniques.[5,22] Any PRM voxel value outside of the 95% confidence interval was classified as a significant increase or decrease in PET tracer uptake.

Region of Interest (ROI) Selection

The current study focused on using contrast enhancing regions on pretreatment, postcontrast T1-weighted images for subsequent PRM analysis. Regions of T2 or FLAIR signal abnormality are thought to encompass the largest extent of malignant infiltrating tumor;[23–27] however, these regions also contain a large fraction of edematous tissue and have traditionally had worse clinical sensitivity than regions of contrast enhancement when evaluating response to bevacizumab.[4] Therefore, regions of contrast enhancement on pretreatment postcontrast images were used in the current study to isolate PRM analysis to regions believed to contain the most aggressive tumor.[28–33] Regions of contrast enhancement are largely accepted as the best measure of tumor burden, because they are used in both standard radiographic assessment (i.e., Macdonald criteria[34]) and the new Response Assessment in Neuro-Oncology assessment.[35] A semiautomated thresholding technique described previously was used to mask the pretreatment contrast-enhancing lesion for each patient.[6] For each PET PRM (4 per patient consisting of a Pre/Post ^{18}F-FDOPA PRM, Post1/Post2 ^{18}F-FDOPA PRM, Pre/Post ^{18}F-FLT PRM, and a Post1/Post2 ^{18}F-FLT PRM), the total volume of increasing [$Vol(+)$], decreasing [$Vol(-)$], or changing (increasing or decreasing [$Vol(+/-)$]) uptake, and the percentage of contrast-enhancing tumor significantly increasing [$\%Vol(+)$], decreasing [$\%Vol(-)$], or changing [$\%Vol(+/-)$] was calculated. Of note, Pre/Post PRMs were defined only with respect to the pretreatment and first posttreatment time point and not between pretreatment and the second posttreatment time point.

Definition of Disease Progression

Progression was defined prospectively by the treating neuro-oncologists. If subsequent scans showed definite increase in imaging-evaluable tumor (≥25% increase in the sum of enhancing lesions, new enhancing lesions >1 cm^2, or an unequivocal qualitative increase in nonenhancing tumor or unequivocal new area of noncontrast enhancing tumor), progression was declared at that time. Change in steroid dosage was taken into consideration while defining progression. Patients who did not meet these imaging criteria for progression but had significant neurologic decline were declared to have progressed at the time of irreversible decline. Patients who died before evidence of imaging progression were defined to have progressed on the date of death. PFS was defined as the time from the start of bevacizumab treatment to radiographic and/or clinical progression. OS was defined as the interval from the start of bevacizumab treatment to patient death.

Hypothesis Testing

Receiver-operating characteristic (ROC) analysis was performed on PET PRM measurements and change in the volume of contrast enhancement on post-contrast T1-weighted images to determine the sensitivity and specificity of detecting 3-month PFS and 6-month OS. Area under the curve (AUC) was used as a measure of PET PRM performance. In addition, survival analysis was performed using log-rank statistical analysis of Kaplan-Meier data. All statistical tests were performed using GraphPad Prism, version 4.0 (GraphPad Software).

Results

After normalization of each PET SUV image to the mean uptake in NAWM, voxel-wise changes in ^{18}F-FDOPA and ^{18}F-FLT in NAWM were quantified to evaluate for temporal stability. The 95% confidence interval for voxel-wise changes in normalized ^{18}F-FDOPA within

NAWM was −14.5% to +14.5% between the pre- and posttreatment time points and −13.5% to +14.5% between the 2 posttreatment time points (Fig. 2A), whereas the 95% confidence interval for voxel-wise changes in normalized ^{18}F-FLT was −29.6% to +34.6% between the pre- and posttreatment time points and −28.6% to +38.7% between the 2 posttreatment time points (Fig. 2B). These confidence intervals were then used for production of ^{18}F-FDOPA and ^{18}F-FLT PET PRMs. (Note that the confidence intervals for ^{18}F-FLT PRMs were slightly asymmetric, biased slightly to a subtle decrease in tracer uptake between the different time points.)

Qualitatively, initial administration with bevacizumab resulted in reduction of both contrast enhancement and T2-weighted signal abnormality for most patients. Similarly, ^{18}F-FDOPA and ^{18}F-FLT showed a significant decrease in uptake for the same patients after initial administration of bevacizumab. Between the 2 posttreatment time points, the change in ^{18}F-FDOPA and ^{18}F-FLT uptake varied, with some patients showing stable or further decreasing levels of uptake, whereas other patients had increased uptake between the 2 posttreatment time points. Patients exhibiting continued decrease in ^{18}F-FDOPA or ^{18}F-FLT uptake in contrast enhancing regions on normalized PET PRMs appeared to be more likely to progress later and live longer (Fig. 3), compared with patients with increased uptake (Fig. 4).

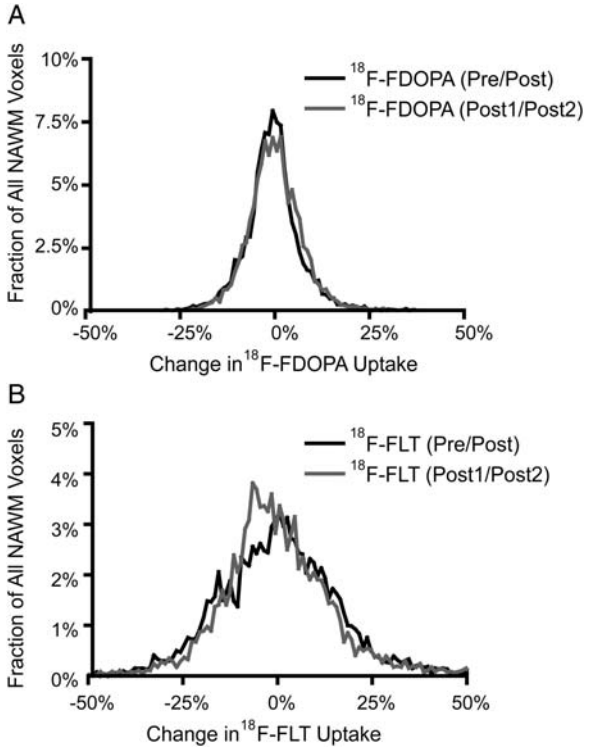

Fig. 2. Pooled histogram data of voxel-wise changes in PET tracer uptake in normal appearing white matter (NAWM) evaluated before and after bevacizumab (Pre/Post) and between the two post-treatment time points (Post1/Post2). (A) Histogram of voxel-wise changes in ^{18}F-FDOPA uptake within NAWM, suggesting the 95% confidence interval ranged from −14.5% to +14.5% (Pre/Post) and −13.5% to +14.5% (Post1/Post2). (B) Histogram of voxel-wise changes in ^{18}F-FLT uptake within NAWM, suggesting the 95% confidence interval ranged from −29.6% to +34.6% (Pre/Post) and −28.6% to 38.7% (Post1/Post2).

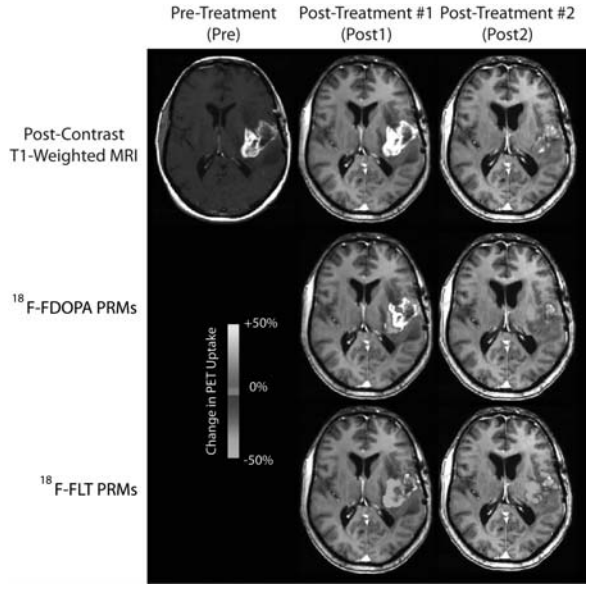

Fig. 3. ^{18}F-FDOPA and ^{18}F-FLT PET PRM responder showing decreased PET uptake after administration of bevacizumab. PFS = 10.6 months, OS = 15 months.

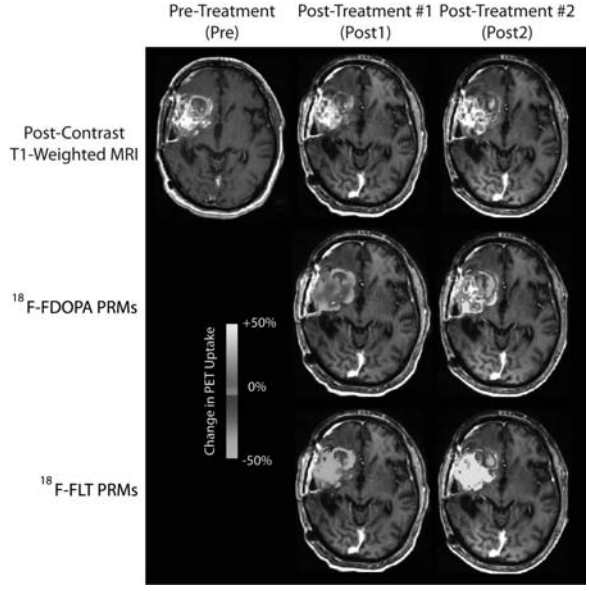

Fig. 4. ^{18}F-FDOPA and ^{18}F-FLT PET PRM non-responder showing increased PET uptake after administration of bevacizumab. PFS = 1.6 months, OS = 3.3 months.

ROC Performance for Predicting 3-Month PFS and 6-Month OS

ROC analysis was performed for each PET PRM metric, along with change in the volume of contrast

enhancement on postcontrast T1-weighted MR images, to determine sensitivity and specificity for predicting 3-month PFS and 6-month OS. Performance of each PET PRM metric for each end point is summarized in Tables 1–4. In general, ROC analysis suggested that a decrease in contrast enhancement of >5cc on MRI before and after treatment was a good predictor of both longer time to progression and overall survival

Table 1. ^{18}F-FDOPA PET PRMs ROC analysis for 3-month progression-free survival (PFS)

Parameter	Threshold	Sensitivity (%)	Specificity (%)	AUC	*P*-Value
$Vol(-)^{Pre/Post}{}_{FDOPA}$ [mL]	7cc	66	45	0.59	0.4884
$Vol(+)^{Pre/Post}{}_{FDOPA}$ [mL]	3cc	66	93	0.70	0.1154
$Vol(+/-)^{Pre/Post}{}_{FDOPA}$ [mL]	**15cc**	**75**	**70**	**0.82**	**0.0110***
$\%Vol(-)^{Pre/Post}{}_{FDOPA}$	38%	56	79	0.54	0.7528
$\%Vol(+)^{Pre/Post}{}_{FDOPA}$	5%	66	79	0.67	0.1859
$\%Vol(+/-)^{Pre/Post}{}_{FDOPA}$	67%	66	57	0.62	0.3447
$Vol(-)^{Post1/Post2}{}_{FDOPA}$ [mL]	3.5cc	75	44	0.56	0.7003
$Vol(+)^{Post1/Post2}{}_{FDOPA}$ [mL]	3cc	56	75	0.54	0.7728
$Vol(+/-)^{Post1/Post2}{}_{FDOPA}$ [mL]	28cc	44	89	0.53	0.8253
$\%Vol(-)^{Post1/Post2}{}_{FDOPA}$	50%	78	50	0.53	0.8474
$\%Vol(+)^{Post1/Post2}{}_{FDOPA}$	3%	78	50	0.61	0.4415
$\%Vol(+/-)^{Post1/Post2}{}_{FDOPA}$	27%	100	33	0.56	0.6911

*$P < .05$.

Table 2. ^{18}F-FDOPA PET PRMs ROC analysis for 6-month overall survival (OS)

Parameter	Threshold	Sensitivity (%)	Specificity (%)	AUC	*P*-Value
$Vol(-)^{Pre/Post}{}_{FDOPA}$ [mL]	20cc	80	50	0.57	0.6056
$Vol(+)^{Pre/Post}{}_{FDOPA}$ [mL]	0.2cc	71	67	0.76	0.0588
$Vol(+/-)^{Pre/Post}{}_{FDOPA}$ [mL]	16cc	67	75	0.65	0.2453
$\%Vol(-)^{Pre/Post}{}_{FDOPA}$	38%	40	75	0.53	0.8465
$\%Vol(+)^{Pre/Post}{}_{FDOPA}$	2%	60	75	0.63	0.3017
$\%Vol(+/-)^{Pre/Post}{}_{FDOPA}$	77%	67	50	0.53	0.8465
$Vol(-)^{Post1/Post2}{}_{FDOPA}$ [mL]	5cc	58	83	0.72	0.1341
$Vol(+)^{Post1/Post2}{}_{FDOPA}$ [mL]	1.5cc	60	67	0.60	0.5121
$Vol(+/-)^{Post1/Post2}{}_{FDOPA}$ [mL]	15cc	67	83	0.71	0.1601
$\%Vol(-)^{Post1/Post2}{}_{FDOPA}$	50%	83	67	0.61	0.4537
$\%Vol(+)^{Post1/Post2}{}_{FDOPA}$	**2.5%**	**91**	**83**	**0.83**	**0.0271***
$\%Vol(+/-)^{Post1/Post2}{}_{FDOPA}$	6%	67	83	0.58	0.5742

*$P < .05$.

Table 3. ^{18}F-FLT PET PRMs ROC analysis for 3-month progression-free survival (PFS)

Parameter	Threshold	Sensitivity (%)	Specificity (%)	AUC	*P*-Value
$Vol(-)^{Pre/Post}{}_{FLT}$ [mL]	7cc	60	40	0.62	0.3211
$Vol(+)^{Pre/Post}{}_{FLT}$ [mL]	0.1cc	70	63	0.60	0.4386
$Vol(+/-)^{Pre/Post}{}_{FLT}$ [mL]	7.5cc	70	35	0.59	0.4568
$\%Vol(-)^{Pre/Post}{}_{FLT}$	70%	90	62	0.70	0.1069
$\%Vol(+)^{Pre/Post}{}_{FLT}$	2%	80	40	0.51	0.9506
$\%Vol(+/-)^{Pre/Post}{}_{FLT}$	**70%**	**90**	**70**	**0.78**	**0.0218***
$Vol(-)^{Post1/Post2}{}_{FLT}$ [mL]	**2cc**	**78**	**78**	**0.81**	**0.0244***
$Vol(+)^{Post1/Post2}{}_{FLT}$ [mL]	4cc	78	56	0.57	0.5963
$Vol(+/-)^{Post1/Post2}{}_{FLT}$ [mL]	8cc	78	78	0.74	0.0852
$\%Vol(-)^{Post1/Post2}{}_{FLT}$	12%	67	78	0.72	0.1223
$\%Vol(+)^{Post1/Post2}{}_{FLT}$	10%	78	78	0.68	0.1854
$\%Vol(+/-)^{Post1/Post2}{}_{FLT}$	30%	56	89	0.66	0.2333

*$P < .05$.

Table 4. ^{18}F-FLT PET PRMs ROC analysis for 6-month overall survival (OS)

Parameter	Threshold	Sensitivity (%)	Specificity (%)	AUC	*P*-value
$Vol(-)^{Pre/Post}{}_{FLT}$ [mL]	7.5cc	54	67	0.51	**0.9380**
$Vol(+)^{Pre/Post}{}_{FLT}$ [mL]	0.3cc	75	80	0.81	**0.0390***
$Vol(+/-)^{Pre/Post}{}_{FLT}$ [mL]	8cc	67	63	0.55	**0.6986**
$\%Vol(-)^{Pre/Post}{}_{FLT}$	22%	88	43	0.53	**0.8411**
$\%Vol(+)^{Pre/Post}{}_{FLT}$	1%	73	67	0.70	**0.1612**
$\%Vol(+/-)^{Pre/Post}{}_{FLT}$	68%	73	75	0.67	**0.1968**
$Vol(-)^{Post1/Post2}{}_{FLT}$ [mL]	6cc	71	50	0.57	**0.6710**
$Vol(+)^{Post1/Post2}{}_{FLT}$ [mL]	3cc	58	75	0.54	**0.7906**
$Vol(+/-)^{Post1/Post2}{}_{FLT}$ [mL]	9cc	64	75	0.64	**0.3956**
$\%Vol(-)^{Post1/Post2}{}_{FLT}$	1%	60	50	0.55	**0.7500**
$\%Vol(+)^{Post1/Post2}{}_{FLT}$	1%	55	50	0.56	**0.6971**
$\%Vol(+/-)^{Post1/Post2}{}_{FLT}$	48%	74	50	0.52	**0.8763**

*$P < .05$.

(Fig. 5A and B; contrast enhancement, 3-month PFS, Sensitivity = 80%, Specificity = 78%, AUC = 0.77, $P = .025$; 6-month OS, Sensitivity = 80%, Specificity = 78%, AUC = 0.78, $P = .033$); however, failure of bevacizumab was at least partially defined by MRI, justifying further inquiry into the predictive nature of PET PRMs.

ROC analysis suggested that a large volume (or volume fraction) of decreased ^{18}F-FDOPA PET uptake was associated with longer PFS and OS. Decreased ^{18}F-FDOPA uptake had a high sensitivity to 3-month PFS and 6-month OS but relatively low specificity. Conversely, the volume (or volume fraction) of increased ^{18}F-FDOPA PET uptake had higher specificity and lower sensitivity for shorter 3-month PFS and 6-month OS. A large volume of voxels with changing ^{18}F-FDOPA uptake within areas of contrast enhancement between pre- and posttreatment time points $[Vol(+/-)^{Pre/Post}{}_{FDOPA}]$ was a statistically significant predictor for 3-month PFS (Table 1; Fig. 5A; Threshold = 15cc, Sensitivity = 75%, Specificity = 70%, AUC = 0.82, $P = .0110$). A volume fraction of increasing ^{18}F-FDOPA uptake within areas of contrast enhancement between the 2 posttreatment time points $[\%Vol(+)^{Post1/Post2}{}_{FDOPA}]$ was a statistically significant predictor of 6-month OS (Table 2; Fig. 5B; Threshold = 2.5%; Sensitivity = 91%; Specificity = 83%, AUC = 0.83, $P = .0271$).

^{18}F-FLT had slightly less specificity for 3-month PFS and 6-month OS than did ^{18}F-DOPA, although overall ROC performance suggested similar trends. Of importance, the volume (and volume fraction) required for ^{18}F-FLT PRMs to predict response was much lower than that required for ^{18}F-FDOPA PRMs. Specifically, the volume fraction of changing voxels in ^{18}F-FLT PRMs evaluated before and after bevacizumab therapy was a significant predictor of 3-month PFS (Table 3; Fig. 5A; Threshold = 70%, Sensitivity = 90%, Specificity = 70%, AUC = 0.78, $P = .0218$). The volume of tissue with decreasing ^{18}F-FLT uptake within regions of contrast enhancing regions on ^{18}F-FLT PRMs was also a significant predictor of 3-month PFS (Table 3; Fig. 5A; Threshold = 2cc, Sensitivity = 78%, Specificity = 78%, AUC = 0.81, $P = .0244$). In addition, increased ^{18}F-FLT uptake in pretreatment contrast-enhancing regions on PRMs evaluated before and after treatment with bevacizumab was a significant predictor of 6-month OS (Table 4; Fig. 5B; Threshold = 0.3cc, Sensitivity = 75%, Specificity = 80%, AUC = 0.81, $P = .0390$).

To evaluate the potential synergy of combining information from both ^{18}F-FDOPA and ^{18}F-FLT scans, we tested whether the sum of tissue with increasing, decreasing, or changing ^{18}F-FDOPA and ^{18}F-FLT and the product of the percentages of enhancing tumor with increasing, decreasing, or changing ^{18}F-FDOPA and ^{18}F-FLT were significant predictors of 3-month PFS or 6-month PFS. The total volume of contrast-enhancing tissue with an increase in ^{18}F-FDOPA and ^{18}F-FLT before and after bevacizumab therapy was a significant predictor of 3-month PFS (Fig. 5C; Threshold = 1cc total volume, Sensitivity = 78%, Specificity = 77%, AUC = 0.80, $P = .018$) but not a predictor of 6-month OS (ROC AUC = 0.61, $P = .413$). Similarly, the total volume of changing ^{18}F-FDOPA and ^{18}F-FLT uptake before and after bevacizumab therapy (Fig. 5C; Threshold = 25cc, Sensitivity = 78%, Specificity = 85%, AUC = 0.79, $P = .021$), the total volume of decreasing ^{18}F-FDOPA and ^{18}F-FLT between the 2 post–bevacizumab therapy scans (Fig. 5C; Threshold = 8cc, Sensitivity = 78%, Specificity = 69%, AUC = 0.75, $P = .049$), and the product of the volume fraction of decreasing ^{18}F-FDOPA and ^{18}F-FLT uptake between the 2 post–bevacizumab therapy scans (Fig. 5C; Threshold = 5%, Sensitivity = 50%, Specificity = 95%, AUC = 0.77, $P = .035$) were significant predictors of 3-month PFS but not 6-month OS.

Survival Analysis

^{18}F-FDOPA PET PRMs were able to stratify patients based on both PFS and OS. In particular, patients exhibiting an increase in ^{18}F-FDOPA uptake >0.35cc (median volume), or 2.5% (median percentage of enhancing tumor), on PRMs from data before and after

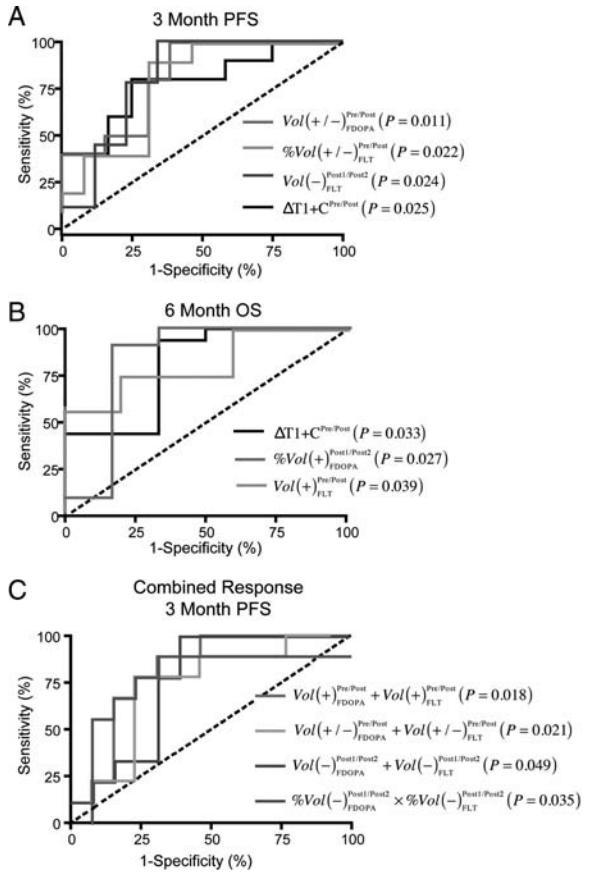

Fig. 5. Best performing PET PRM metrics according to ROC performance for prediction of 3 month PFS and 6 month OS. (A) ROC results of individual PET PRMs (and standard change in contrast enhancement on post-contrast T1-weighted images) to predict 3 month PFS. (B) ROC results for individual PET PRMs (and standard post-contrast T1) to predict 6 month OS. (C) ROC results for combined PET PRM data to predict 3 month PFS. $Vol(+/-)^{Pre/Post}_{FDOPA}$ = total volume of changing voxels on ^{18}F-FDOPA PRMs evaluated before and after first dose of bevacizumab. $\%Vol(+/-)^{Pre/Post}_{FLT}$ = total volume fraction (percentage of pre-treatment enhancing tumor) on ^{18}F-FLT PRMs evaluated before and after first dose of bevacizumab. $Vol(-)^{Post1/Post2}_{FLT}$ = total volume of voxels with decreasing ^{18}F-FLT uptake on PRMs evaluated using the two post-treatment scans. $\Delta T1 + C$ = change in contrast-enhancing volume before and after first dose of bevacizumab. $\%Vol(+)^{Post1/Post2}_{FDOPA}$ = volume fraction of increasing ^{18}F-FDOPA uptake on PRMs evaluated using the two post-treatment scans. $Vol(+)^{Pre/Post}_{FLT}$ = total volume of increasing ^{18}F-FLT uptake on PRMs evaluated before and after initial dose of bevacizumab. Lots of these descriptions can go into the body of results.

bevacizumab treatment were at risk for shorter PFS but not OS (Fig. 6A; $Vol(+)^{Pre/Post}_{FDOPA}$, Log-rank, $P = .0160$; $\%Vol(+)^{Pre/Post}_{FDOPA}$, Log-rank, $P = .0122$). An increase in ^{18}F-FDOPA uptake >5.7% (median) on PRMs from data between the follow-up scans after the initial bevacizumab dose, however, were at risk for shorter PFS and OS (Fig. 6A; PFS, Log-rank, $P = .0182$; Fig. 5B; OS, Log-rank, $P = .0111$). Log-rank analysis on Kaplan-Meier data suggested a volume fraction of increasing ^{18}F-FLT uptake on PRMs evaluated between the 2 follow-up posttreatment time points >10% resulted in a statistically shorter PFS (Fig. 6C; $\%Vol(+)^{Post1/Post2}_{FLT}$, Log-rank, $P = .0035$); however, there was no significant difference in OS between these groups. Combined response of ^{18}F-FDOPA and ^{18}F-FLT PET PRMs allowed for significant separation of PFS using a threshold of 15% (Fig. 6D; $\%Vol(+)^{Pre/Post}_{FDOPA}$ or $\%Vol(+)^{Pre/Post}_{FLT}$, Log-rank, $P = .0010$). This same criterion was not predictive of OS.

Discussion

Results from the current study suggest that a large volume (or volume fraction) of increased ^{18}F-FDOPA or ^{18}F-FLT uptake on PRMs evaluated between the 2 follow-up time points after initial administration of bevacizumab treatment were associated with a shortened PFS, compared with patients with a sustained decrease in uptake after treatment. Decreased uptake in both tracers appeared to provide a high sensitivity but low specificity for predicting 3-month PFS and 6-month OS; conversely, increased uptake was associated with a high specificity and low sensitivity for predicting these same end points. Log-rank analysis revealed, however, that only ^{18}F-FDOPA PRM measurements taken using the 2 posttreatment time points were a statistically significant predictor of OS.

Of note, test-retest reliability of PET tracers in the current study were consistent with previous studies examining PET uptake in normal structures, suggesting that results obtained in the current study may be applicable at other clinical sites. For example, ^{18}F-FDOPA PET uptake in normal individuals has been estimated at approximately 8%.[36] Assuming that ^{18}F-FDOPA SUVs follow a normal distribution, this 8% standard deviation results in a 95% confidence interval for change in ^{18}F-FDOPA SUV of approximately 15%, consistent with estimates in the current study of approximately 14.5%. Standard deviation in ^{18}F-FLT SUV uptake, however, has been estimated to be as high as 15%.[37,38] A standard deviation this high results in a 95% confidence interval for ^{18}F-FLT of nearly 30%, consistent with the voxel-wise 95% confidence interval for NAWM of approximately 30%. Together, these results suggest that the inherent variability in ^{18}F-FDOPA uptake may be slightly less than that of ^{18}F-FLT PET, which may explain the superior performance of ^{18}F-FDOPA PRMs, compared with ^{18}F-FLT PRMs. Of importance, however, the volume (and volume fraction) required for ^{18}F-FDOPA PRMs to predict response was greater than that required for ^{18}F-FLT.

Similar to results from the current study, other voxel-wise biomarkers have shown the ability to predict response to bevacizumab in recurrent malignant gliomas, including the use of functional diffusion maps (fDMs),[4] cell invasion, motility, proliferation level estimate (CIMPLE) maps,[7] and differential quantitative

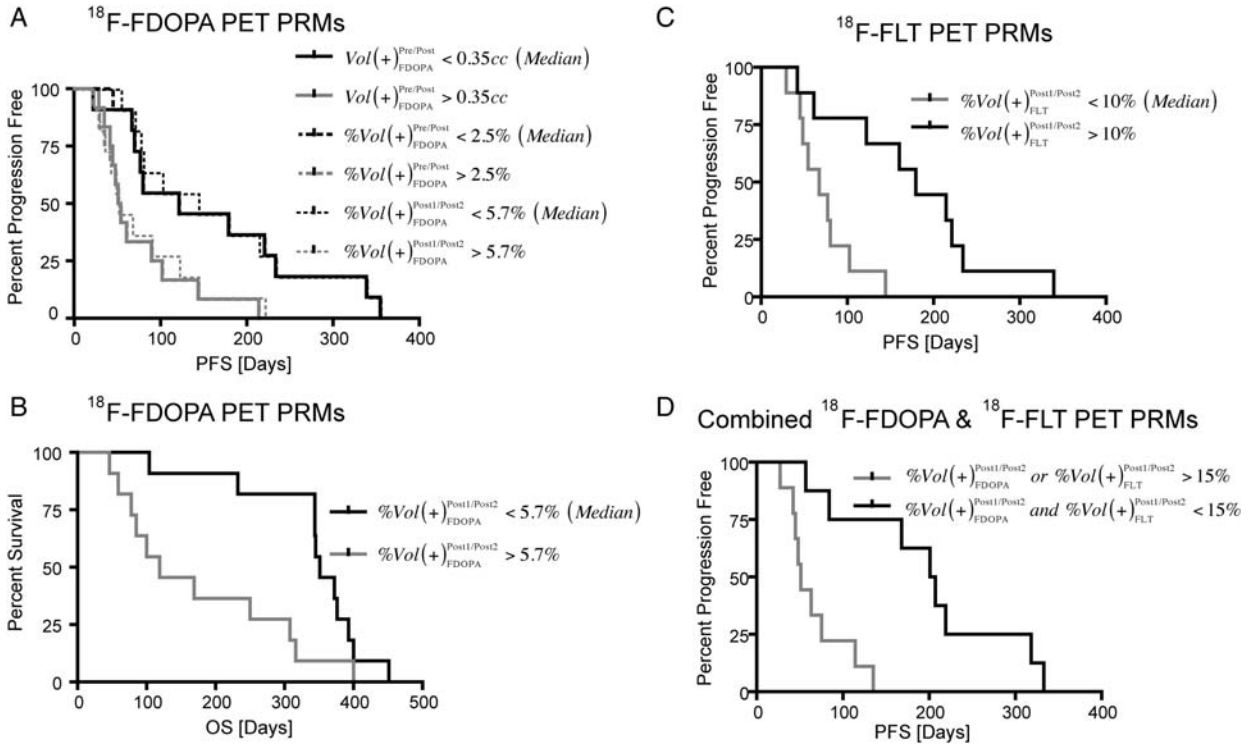

Fig. 6. Best performing ^{18}F-FDOPA and ^{18}F-FLT PET PRM metrics according to Log-rank analysis on Kaplan-Meier survival data. (A) Stratification of short- and long-term PFS using ^{18}F-FDOPA PET PRMs. (B) Stratification of short- and long-term OS using ^{18}F-FDOPA PET PRMs. (C) Stratification of short- and long-term PFS using ^{18}F-FLT PET PRMs. (D) Further stratification of short- and long-term PFS using the combined ^{18}F-FDOPA and ^{18}F-FLT PET PRM response. All PET PRM metrics shown had statistically significant separation according to Log-rank analysis ($P < .05$).

T2 (DQT2) maps.[5] Studies examining fDMs and DQT2 demonstrated significant changes in the apparent diffusion coefficient (ADC) and T2 relaxation rate, which was largely attributed to changes in vascular permeability and edema. CIMPLE maps, which were evaluated after administration of bevacizumab, were thought to more closely reflect changes in cell proliferation rate rather than changes in edema. It is conceivable that the large decrease in tracer uptake observed before and after initial administration of bevacizumab in the current study was attributable to the change in vascular permeability or perfusion, whereas the change in tumor uptake between the 2 posttreatment follow-up time points more closely reflected changes in tumor metabolism and proliferation. Muzi et al.[39] clearly demonstrated the dependence of ^{18}F-FLT uptake rate (i.e., K_1) on vascular permeability; however, studies have shown that ^{18}F-FDOPA uptake rate may not reflect simple tracer diffusion because of disruption of the blood-brain barrier but, instead, likely reflects the rate of carrier-mediated facilitated transportation.[40] In direct contrast with the notion that the effects found in the current study were directly attributable to changes in permeability, we observed regions of increased and decreased PET uptake in areas of residual contrast enhancement after treatment with bevacizumab. Despite this evidence, future studies examining the effects of vascular permeability on ^{18}F-FDOPA and ^{18}F-FLT uptake are warranted.

Although both MRI and PET may be predictive of response to therapy, they provide dramatically different information about tumor biology. Although a change in contrast-enhancing volume as a result of therapy was predictive of PFS and OS, a change in PET uptake on subsequent time points (excluding the potential confounds from vascular permeability) was a better predictor of PFS. These results suggest that MRI and PET features are distinctly different and are both potentially valuable. Of note, although change in contrast-enhancing volume before and after bevacizumab treatment was predictive of 3-month PFS, progression was at least partially defined by contrast enhancement via MRI, potentially introducing bias into this type of analysis. Furthermore, the study performed by Schwarzenberg et al,[13] which used the same patients but evaluated using ROI analysis, also found that MRI was predictive of PFS and OS; however, PET analysis provided increased predictive power, compared with MRI alone.

Previous studies have shown that changes in ^{18}F-FLT SUV are a useful tool for predicting PFS and OS in recurrent malignant gliomas treated with bevacizumab;[13,14] however, static SUV measurements at a single time point were not predictive of response. Similar to these studies, the PRM technique applied to ^{18}F-FLT data was able to stratify patients according to PFS and provided more localized qualitative information of changes in tracer uptake around the tumor region. The current study, however, did not find a statistical relationship

between ^{18}F-FLT uptake and OS when using the Kaplan-Meier analysis. This is likely to be attributable to the relatively wide confidence intervals for voxel-wise change in ^{18}F-FLT uptake in NAWM, compared with ^{18}F-FDOPA uptake (Fig. 2). This high variability resulted in fewer voxels being categorized as significantly increasing or decreasing and may have lowered the overall sensitivity of this biomarker for stratifying OS. Future studies aimed at either reducing this variability or using a different confidence interval for ^{18}F-FLT PRMs may be necessary for improving performance of this biomarker.

In addition to ^{18}F-FLT, kinetic parameters and uptake measured by SUVs of ^{18}F-FDOPA have been previously studied for the prediction of tumor grade and proliferative activity in glioblastoma.[12,15,41,42] However, to our knowledge, ^{18}F-FDOPA has not previously been tested for predictive capabilities of PFS and OS among patients with recurrent malignant gliomas treated with bevacizumab. The current study demonstrates that voxel-wise changes in ^{18}F-FDOPA provided higher sensitivity and specificity for predicting 3-month PFS and 6-month OS and allowed statistically significant separation of short- and long-term PFS and OS using log-rank analysis.

Although the current study used ^{18}F-FDOPA and ^{18}F-FLT PET images to predict the response to recurrent malignant gliomas treated with bevacizumab, other PET tracers have also shown promise for predicting response to anti-angiogenic therapy. For example, a recent study by Colavolpe et al.[43] clearly demonstrated the prognostic ability of baseline, pretreatment ^{18}F-FDG maximum SUV to predict the response to bevacizumab and irinotecan therapy in malignant gliomas, supporting the hypothesis that ^{18}F-FDG uptake is strongly correlated with angiogenesis markers in gliomas.[44] Median ^{18}F-FDG SUV in contrast-enhancing regions, normalized to gray matter, at 4 weeks posttreatment has also been shown to be a significant prognostic factor in anaplastic gliomas treated with single-agent bevacizumab;[45] however, this study did not find baseline or change in ^{18}F-FDG PET uptake to be particularly predictive of patient response. On the basis of these somewhat conflicting results, which are likely to be attributable to different definitions of ^{18}F-FDG uptake and slightly different patient populations, we hypothesize that ^{18}F-FDG PET PRMs may also be useful for assessing malignant glioma response to bevacizumab.

Study Limitations

One inherent source of error in PRM analysis is imperfect registration between MR and PET images acquired separately and with registration of MR and PET images in the same patient over multiple time points. This misregistration is often attributable to mass effect related to tumor growth. Another potential source of error is the normalization process. Specifically, normalization of PET activity values based on contralateral white matter may have skewed our results because of inter-patient variations in local tracer uptake. Our investigations suggested that a form of normalization was necessary, because we found a significant difference in SUV value in regions of NAWM in the same patient over time. By normalizing to the SUV in NAWM, the variability of measurements in normal regions in brain for the same patient across time was largely reduced, allowing us to more accurately characterize subtle changes in tracer uptake in the tumor regions.

As has been demonstrated in ^{18}F-FDOPA evaluation of patients with movement disorders affecting the striatal dopamine pathway,[46,47] the basal ganglia has intrinsic uptake of ^{18}F-FDOPA through neutral amino acid transporters.[48] Thus, ^{18}F-FDOPA PET may have an inherent limitation for evaluation of subcortical tumors near the basal ganglia. However, ^{18}F-FDOPA PET PRMs quantify the change in ^{18}F-FDOPA uptake in tumor regions; therefore, this potential limitation may not be substantial.

Lastly, we chose to use regions of contrast enhancement on postcontrast MR images prior to treatment with bevacizumab as regions of interest for the current analysis. Previous studies suggested that regions of FLAIR signal abnormality may also be beneficial to examine, because FLAIR regions may contain metabolically active areas of nonenhancing tumor. Although not shown in the current study, PRM analysis of PET tracers in FLAIR regions was largely not informative beyond that of postcontrast ROIs. Future studies aimed at improving these limitations are necessary to fully understand the capabilities of quantitative PET PRMs.

Conclusion

The current study examined retrospective ^{18}F-FDOPA and ^{18}F-FLT PET data collected from 24 patients with recurrent malignant gliomas treated with bevacizumab to construct voxel-wise PET PRMs. PRMs provided a visual and quantitative assessment of regional changes in PET uptake and prognostic information about PFS based on change in tracer uptake during the weeks after treatment. Despite these promising findings, we observed only a weak relationship between PRM response and OS. These results suggest that ^{18}F-FDOPA and ^{18}F-FLT PET PRM may be valuable imaging biomarkers for predicting PFS in recurrent malignant gliomas treated with bevacizumab.

Acknowledgments

Authors Wei Chen and Benjamin M. Ellingson contributed equally to this work.

Conflict of interest statement. None declared.

Funding

This work was supported by UCLA Institute for Molecular Medicine Seed Grant (to B.M.E.), UCLA Radiology Exploratory Research Grant (to B.M.E.), Art of the Brain (to T.F.C.), Ziering Family Foundation in memory of Sigi Ziering (to T.F.C.), Singleton Family Foundation (to T.F.C.), and Clarence Klein Fund for Neuro-Oncology (to T.F.C.).

References

1. Weil RJ. Glioblastoma multiforme–treating a deadly tumor with both strands of RNA. *PLoS Med*. 2006;3(1):e31.
2. Chamberlain MC. Emerging clinical principles on the use of bevacizumab for the treatment of malignant gliomas. *Cancer*. 2010;116(17):3988–3999.
3. Nghiemphu PL, Liu W, Lee Y, et al. Bevacizumab and chemotherapy for recurrent glioblastoma: a single-institution experience. *Neurology*. 2009;72(14):1217–1222.
4. Ellingson BM, Cloughesy TF, Lai A, et al. Graded functional diffusion map-defined characteristics of apparent diffusion coefficients predict overall survival in recurrent glioblastoma treated with bevacizumab. *Neuro Oncol*. 2011;13(10):1151–1161.
5. Ellingson BM, Cloughesy TF, Lai A, et al. Quantification of edema reduction using differential quantitative T2 (DQT2) relaxometry mapping in recurrent glioblastoma treated with bevacizumab. *J Neurooncol*. 2012;106(1):111–119.
6. Ellingson BM, Cloughesy TF, Lai A, Nghiemphu PL, Mischel PS, Pope WB. Quantitative volumetric analysis of conventional MRI response in recurrent glioblastoma treated with bevacizumab. *Neuro Oncol*. 2011;13(4):401–409.
7. Ellingson BM, Cloughesy TF, Lai A, Nghiemphu PL, Pope WB. Cell invasion, motility, and proliferation level estimate (CIMPLE) maps derived from serial diffusion MR images in recurrent glioblastoma treated with bevacizumab. *J Neurooncol*. 2011;105(1):91–101.
8. Pope WB, Lai A, Mehta R, et al. Apparent diffusion coefficient histogram analysis stratifies progression-free survival in newly diagnosed bevacizumab-treated glioblastoma. *AJNR Am J Neuroradiol*. 2011;32(5):882–889.
9. Pope WB, Kim HJ, Huo J, et al. Recurrent glioblastoma multiforme: ADC histogram analysis predicts response to bevacizumab treatment. *Radiology*. 2009;252(1):182–189.
10. Hong IK, Kim JH, Ra YS, Kwon do H, Oh SJ, Kim JS. Diagnostic Usefulness of 3′-Deoxy-3′-[18F]Fluorothymidine Positron Emission Tomography in Recurrent Brain Tumor. *J Comput Assist Tomogr*. 2011;35(6):679–684.
11. Chen W, Cloughesy T, Kamdar N, et al. Imaging proliferation in brain tumors with 18F-FLT PET: comparison with 18F-FDG. *J Nucl Med*. 2005;46(6):945–952.
12. Gonzalez-Forero M, Prieto E, Dominguez I, Vigil C, Penuelas I, Arbizu J. [Dual time point 18F-FDOPA PET as a tool for characterizing brain tumors]. *Rev Esp Med Nucl*. 2011;30(2):88–93.
13. Schwarzenberg J, Czernin J, Cloughesy TF, et al. 3′-Deoxy-3′-18F-Fluorothymidine PET and MRI for Early Survival Predictions in Patients with Recurrent Malignant Glioma Treated with Bevacizumab. *J Nucl Med*. 2012;53(1):29–36.
14. Chen W, Delaloye S, Silverman DH, et al. Predicting treatment response of malignant gliomas to bevacizumab and irinotecan by imaging proliferation with [18F] fluorothymidine positron emission tomography: a pilot study. *J Clin Oncol*. 2007;25(30):4714–4721.
15. Fueger BJ, Czernin J, Cloughesy T, et al. Correlation of 6–18F-fluoro-L-dopa PET uptake with proliferation and tumor grade in newly diagnosed and recurrent gliomas. *J Nucl Med*. 2010;51(10):1532–1538.
16. Ledezma CJ, Chen W, Sai V, et al. 18F-FDOPA PET/MRI fusion in patients with primary/recurrent gliomas: initial experience. *Eur J Radiol*. 2009;71(2):242–248.
17. Chen W, Silverman DH, Delaloye S, et al. 18F-FDOPA PET imaging of brain tumors: comparison study with 18F-FDG PET and evaluation of diagnostic accuracy. *J Nucl Med*. 2006;47(6):904–911.
18. Namavari M, Bishop A, Satyamurthy N, Bida G, Barrio JR. Regioselective radiofluorodestannylation with [18F]F2 and [18F]CH3COOF: a high yield synthesis of 6-[18F]Fluoro-L-dopa. *Int J Rad Appl Instrum A*. 1992;43(8):989–996.
19. Bishop A, Satyamurthy N, Bida G, Hendry G, Phelps M, Barrio JR. Proton irradiation of [18O]O2: production of [18F]F2 and [18F]F2 + [18F] OF2. *Nucl Med Biol*. 1996;23(3):189–199.
20. Blocher A, Kuntzsch M, Wei R, Machulla HJ. Synthesis and labeling of 5′-O-(4,4′-dimethoxytrityl)-2,3′-anhydrothymidine for [F-18]FLT preparation. *J Radioanal Nucl Chem.* 2002;251(1):55–58.
21. Bergstrom M, Litton J, Eriksson L, Bohm C, Blomqvist G. Determination of object contour from projections for attenuation correction in cranial positron emission tomography. *J Comput Assist Tomogr*. 1982;6(2):365–372.
22. Ellingson BM, Malkin MG, Rand SD, et al. Validation of functional diffusion maps (fDMs) as a biomarker for human glioma cellularity. *J Magn Reson Imaging*. 2010;31(3):538–548.
23. Brant-Zawadzki M, Norman D, Newton TH, et al. Magnetic resonance of the brain: the optimal screening technique. *Radiology*. 1984;152(1):71–77.
24. Byrne TN. Imaging of gliomas. *Semin Oncol*. 1994;21(2):162–171.
25. Husstedt HW, Sickert M, Kostler H, Haubitz B, Becker H. Diagnostic value of the fast-FLAIR sequence in MR imaging of intracranial tumors. *Eur Radiol*. 2000;10(5):745–752.
26. Tsuchiya K, Mizutani Y, Hachiya J. Preliminary evaluation of fluid-attenuated inversion-recovery MR in the diagnosis of intracranial tumors. *AJNR Am J Neuroradiol*. 1996;17(6):1081–1086.
27. Essig M, Hawighorst H, Schoenberg SO, et al. Fast fluid-attenuated inversion-recovery (FLAIR) MRI in the assessment of intraaxial brain tumors. *J Magn Reson Imaging*. 1998;8(4):789–798.
28. Lewander R, Bergstrom M, Bergvall U. Contrast enhancement of cranial lesions in computed tomography. *Acta Radiol Diagn (Stockh)*. 1978;19(4):529–552.
29. Greene GM, Hitchon PW, Schelper RL, Yuh W, Dyste GN. Diagnostic yield in CT-guided stereotactic biopsy of gliomas. *J Neurosurg*. 1989;71(4):494–497.
30. Kelly PJ, Daumas-Duport C, Kispert DB, Kall BA, Scheithauer BW, Illig JJ. Imaging-based stereotaxic serial biopsies in untreated intracranial glial neoplasms. *J Neurosurg*. 1987;66(6):865–874.
31. Kelly PJ. Computed tomography and histologic limits in glial neoplasms: tumor types and selection for volumetric resection. *Surg Neurol*. 1993;39(6):458–465.
32. Earnest FT, Kelly PJ, Scheithauer BW, et al. Cerebral astrocytomas: histopathologic correlation of MR and CT contrast enhancement with stereotactic biopsy. *Radiology*. 1988;166(3):823–827.
33. Watanabe M, Tanaka R, Takeda N. Magnetic resonance imaging and histopathology of cerebral gliomas. *Neuroradiology*. 1992;34(6):463–469.
34. Macdonald DR, Cascino TL, Schold SC, Jr., Cairncross JG. Response criteria for phase II studies of supratentorial malignant glioma. *J Clin Oncol*. 1990;8(7):1277–1280.
35. Wen PY, Macdonald DR, Reardon DA, et al. Updated response assessment criteria for high-grade gliomas: response assessment in neuro-oncology working group. *J Clin Oncol*. 2010;28(11):1963–1972.
36. Vingerhoets FJ, Snow BJ, Schulzer M, et al. Reproducibility of fluorine-18–6-fluorodopa positron emission tomography in normal human subjects. *J Nucl Med*. 1994;35(1):18–24.

37. de Langen AJ, Klabbers B, Lubberink M, et al. Reproducibility of quantitative 18F-3′-deoxy-3′-fluorothymidine measurements using positron emission tomography. *Eur J Nucl Med Mol Imaging*. 2009;36(3):389–395.
38. Shields AF, Lawhorn-Crews JM, Briston DA, et al. Analysis and reproducibility of 3′-Deoxy-3′-[18F]fluorothymidine positron emission tomography imaging in patients with non-small cell lung cancer. *Clin Cancer Res*. 2008;14(14):4463–4468.
39. Muzi M, Spence AM, O'Sullivan F, et al. Kinetic analysis of 3′-deoxy-3′-18F-fluorothymidine in patients with gliomas. *J Nucl Med*. 2006;47(10):1612–1621.
40. Huang SC, Yu DC, Barrio JR, et al. Kinetics and modeling of L-6-[18F]fluoro-dopa in human positron emission tomographic studies. *J Cereb Blood Flow Metab*. 1991;11(6):898–913.
41. Tripathi M, Sharma R, D'Souza M, et al. Comparative evaluation of F-18 FDOPA, F-18 FDG, and F-18 FLT-PET/CT for metabolic imaging of low grade gliomas. *Clin Nucl Med*. 2009;34(12):878–883.
42. Dowson N, Bourgeat P, Rose S, et al. Joint factor and kinetic analysis of dynamic FDOPA PET scans of brain cancer patients. *Med Image Comput Comput Assist Interv*. 2010;13(Pt 2):185–192.
43. Colavolpe C, Chinot O, Metellus P, et al. FDG-PET predicts survival in recurrent high-grade gliomas treated with bevacizumab and irinotecan. *Neuro Oncol*. 2012;14(5):649–657.
44. Cher LM, Murone C, Lawrentschuk N, et al. Correlation of hypoxic cell fraction and angiogenesis with glucose metabolic rate in gliomas using 18F-fluoromisonidazole, 18F-FDG PET, and immunohistochemical studies. *J Nucl Med*. 2006;47(3):410–418.
45. Kreisl TN, Zhang W, Odia Y, et al. A phase II trial of single-agent bevacizumab in patients with recurrent anaplastic glioma. *Neuro Oncol*. 2011;13(10):1143–1150.
46. Garnett S, Firnau G, Nahmias C, Chirakal R. Striatal dopamine metabolism in living monkeys examined by positron emission tomography. *Brain Res*. 1983;280(1):169–171.
47. Garnett ES, Firnau G, Nahmias C. Dopamine visualized in the basal ganglia of living man. *Nature*. 1983;305(5930):137–138.
48. Yee RE, Cheng DW, Huang SC, Namavari M, Satyamurthy N, Barrio JR. Blood-brain barrier and neuronal membrane transport of 6-[18F]fluoro-L-DOPA. *Biochem Pharmacol*. 2001;62(10):1409–1415.